Nanoscale Advances

ROYAL SOCIETY OF CHEMISTRY

PAPER

View Article Online
View Journal | View Issue

Cite this: *Nanoscale Adv.*, 2022, **4**, 3883

Aerolysin nanopore-based identification of proteinogenic amino acids using a bipolar peptide probe†

Yaxian Ge,[a] Mengjie Cui,[a] Qiuqi Zhang,[b] Ying Wang*[a] and Dongmei Xi *[a]

Received 29th March 2022
Accepted 5th August 2022

DOI: 10.1039/d2na00190j

rsc.li/nanoscale-advances

Nanopore technology has attracted extensive attention due to its rapid, highly sensitive, and label-free performance. In this study, we aimed to identify proteinogenic amino acids using a wild-type aerolysin nanopore. Specifically, bipolar peptide probes were synthesised by linking four aspartic acid residues to the N-terminal and five arginine residues to the C-terminal of individual amino acids. With the help of the bipolar peptide carrier, 9 proteinogenic amino acids were reliably recognised based on current blockade and dwell time using an aerolysin nanopore. Furthermore, by changing the charge of the peptide probe, two of the five unrecognized amino acids above mentioned were identified. These findings promoted the application of aerolysin nanopores in proteinogenic amino acid recognition.

Introduction

Nanopores have proven to be an attractive and powerful platform in the single-molecule analysis.[1–5] Over the past two decades, they have been explored for a wide range of applications including DNA sequencing,[6–8] analysis of the structure of peptides,[9–11] dynamics of peptide transport,[12–15] conformational changes of proteins,[16,17] unfolding[18–20] and folding of proteins,[21,22] and application of disease detection.[23,24] In this rapidly evolving field, it is hoped that nanopore technology can make a breakthrough in the determination of protein primary structure. However, there are 20 amino acids that make up proteins, and nanopore technology is more challenging to identify individual amino acids than single bases.[25–28] Recently, an aerolysin nanopore was used to enable size discrimination of short uniformly charged arginine peptides at a single amino acid resolution by virtue of its high spatial resolution.[29] Furthermore, H. Ouldali *et al.* demonstrated a strategy that allowed the identification of 13 of the 20 unmodified amino acids in an aerolysin nanopore using a short polycationic carrier, and 2 amino acids upon chemical modification.[30] In the absence of any modification or labelling, a single cysteine molecule produced distinctive current blockage, while asparagine or glutamine with large volumes caused unrecognized current blockage.[31] A T232K/K238Q mutant aerolysin nanopore could identify unphosphorylated Tau with almost 100% accuracy by changing the charge of amino acid sites.[32] All these advancements indicate that the aerolysin nanopore holds great potential for identification of proteinogenic amino acids.

Polypeptide is a good carrier for amino acid recognition. The bipolar peptide probe structure was first developed by Asandei *et al.* (2015), and they demonstrated that the positively and negatively charged tails of the bipolar peptide produce a tug-of-war effect after entering the nanopore under the action of the electric field, which may increase its residence time in the nanopore and help to identify the target amino acid.[33–35] Inspired by this, we designed a bipolar peptide probe aimed to identify proteinogenic amino acids using a wild-type aerolysin nanopore. The N-terminus of the amino acid was chemically linked to a peptide with aspartic acid residues (D) and the C-terminus of the amino acid was chemically connected to a peptide with arginine residues (R) to form bipolar peptide probes. In this case, the peptide probe had a strong negatively charged N-terminus and a strong positively charged C-terminus at neutral pH. With this probe, we demonstrated the identification of 9 amino acids using the aerolysin nanopore without any chemical or physical modifications. Our efforts will help in proteinogenic amino acid recognition by the aerolysin nanopore.

Experimental

Reagents and chemicals

1,2-Diphytanoyl-*sn*-glycero-3-phosphocholine was purchased from Avanti Polar Lipids, Inc. (Alabaster, AL, USA). Pro-aerolysin was kindly provided by Professor Yi-Tao Long (East China University of Science and Technology). Trypsin-EDTA, potassium chloride, and decane were purchased from Sigma-Aldrich

[a]*Shandong Provincial Key Laboratory of Detection Technology for Tumor Markers, College of Life Science, Linyi University, Linyi 276005, P. R. China. E-mail: dongmxi@126.com; m13854869219@163.com*

[b]*The First School of Clinical Medicine, Southern Medical University, Guangzhou 510515, P. R. China*

† Electronic supplementary information (ESI) available. See https://doi.org/10.1039/d2na00190j

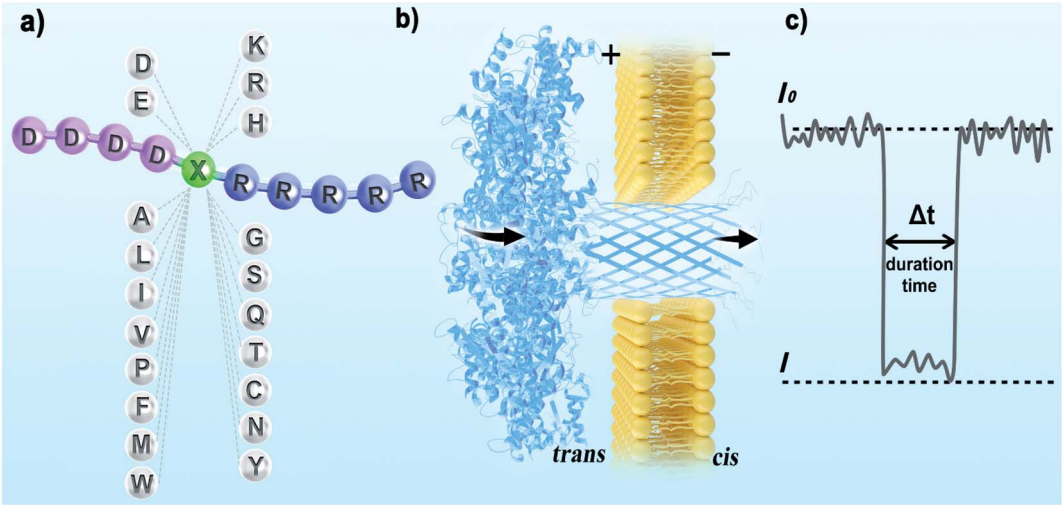

Fig. 1 Schematic diagram for identifying proteinogenic amino acids using an aerolysin nanopore. (a) Schematic representation of the peptide probe with proteinogenic amino acids. A peptide with five arginine residues was chemically linked to the carboxyl end of target amino acid X, and a peptide with four aspartic acid residues was added to the amino terminus of target amino acid X. X represents any one of the 20 proteinogenic amino acids. A total of 20 bipolar D_4XR_5 peptides were formed. (b) Schematic representation of the experimental setup (not to scale). An external voltage of +70 mv was applied on the *trans* side of the bilayer, and the *cis* side was located at the voltage ground. (c) Illustration of a typical current blockade.

Co., Ltd (St Louis, MO, USA). The reagents and materials used in this study were of analytical grade. All peptide samples were synthesised and purified by high-performance liquid chromatography at GL Biochem Ltd (Shanghai, China). The sequences of peptides in the assay are shown in Table S1.† All solutions were prepared using ultrapure water (18.2 MΩ cm at 25 °C) obtained using the Milli-Q Academic A10 system (EMD Millipore, Billerica, MA, USA).

Nanopore electrical recording

Pro-aerolysin was digested with trypsin for 6 h at room temperature. The pro-peptide sequence of pro-aerolysin was completely degraded, and then aerolysin was released.[30] 1,2-Diphytanoyl-*sn*-glycero-3-phosphocholine was dissolved in decane solution to obtain a final concentration of 50 mg L^{-1} and then added to the *trans* chamber in a Delrin bilayer cup (Warner Instruments, Hamden, CT). After forming a lipid bilayer, aerolysin was inserted into the lipid bilayer to obtain a final concentration of 1.0 μg mL^{-1}, which partitioned the aperture into a *cis* chamber and a *trans* chamber. The electrolyte solutions in the *cis* and *trans* chambers of the lipid bilayer were buffered with tris-EDTA (10 mM tris, 1 mM EDTA, 3.0 M KCl, pH 7.5). The pore insertion was identified upon observing a well-defined leap of current values.[29] Once a stable single-pore insertion was detected, the bipolar peptide was added near the newly formed nanopore in the *trans* chamber at a final concentration of 2 μM. The room temperature was maintained at 25 ± 2 °C for this assay, and the error represented the standard deviation of three independent experiments. In the detection process through the aerolysin nanopore, the distinct characteristics of each bipolar peptide were recorded, including current blockades, dwell times, and signal shape under the same experimental conditions.

Data analysis

The current recordings were measured with a patch-clamp amplifier (Axon 200 B, AXON, USA) and converted into data using a DigiData 1440A converter (Molecular Devices, Danaher, USA). The signals were filtered at 5 kHz and acquired at a sampling rate of 100 kHz using PClamp 10.6 (Axon Instruments, Forest City, CA, USA). Finally, the data were analysed using Matlab (R2013b, MathWorks, Natick, MA, USA) software, OriginLab 9.0 (OriginLab Corporation, Northampton, MA, USA), and programs that were developed by Long's group.[36,37] Typically, more than 1000 blockade events are collected in each ionic current measurement. The original ABF file data of the nanopore experiment is converted to TXT files using the Cutting software programmed by Long's group. Then the TXT files are processed using Matlab, the current signals through the nanopore are screened. The screened data are imported into OriginLab 9.0 for function fitting, and the scatter plot, blocking degree and duration time can be obtained respectively. From the current blockades corresponding to each peptide, the mean blockade degree and duration are calculated for each peptide. The mean blockade degree and duration correspond to the arithmetic mean of the blockade degree and durations, respectively. The error bar is calculated using the "Statistics" function of OriginLab 9.0.

Identification of proteinogenic amino acids

The peptide powder was incubated with ultrapure water at room temperature for 30 min. Before nanopore evaluation, the peptide was dissolved in a buffer containing 3 M KCl, 10 mM Tris, and 1 mM EDTA at pH 7.5 to a final concentration of 2 μM. Unless otherwise specified, the nanopore experiments in the assay were performed at a constant voltage of +70 mV applied to the *trans* compartment.

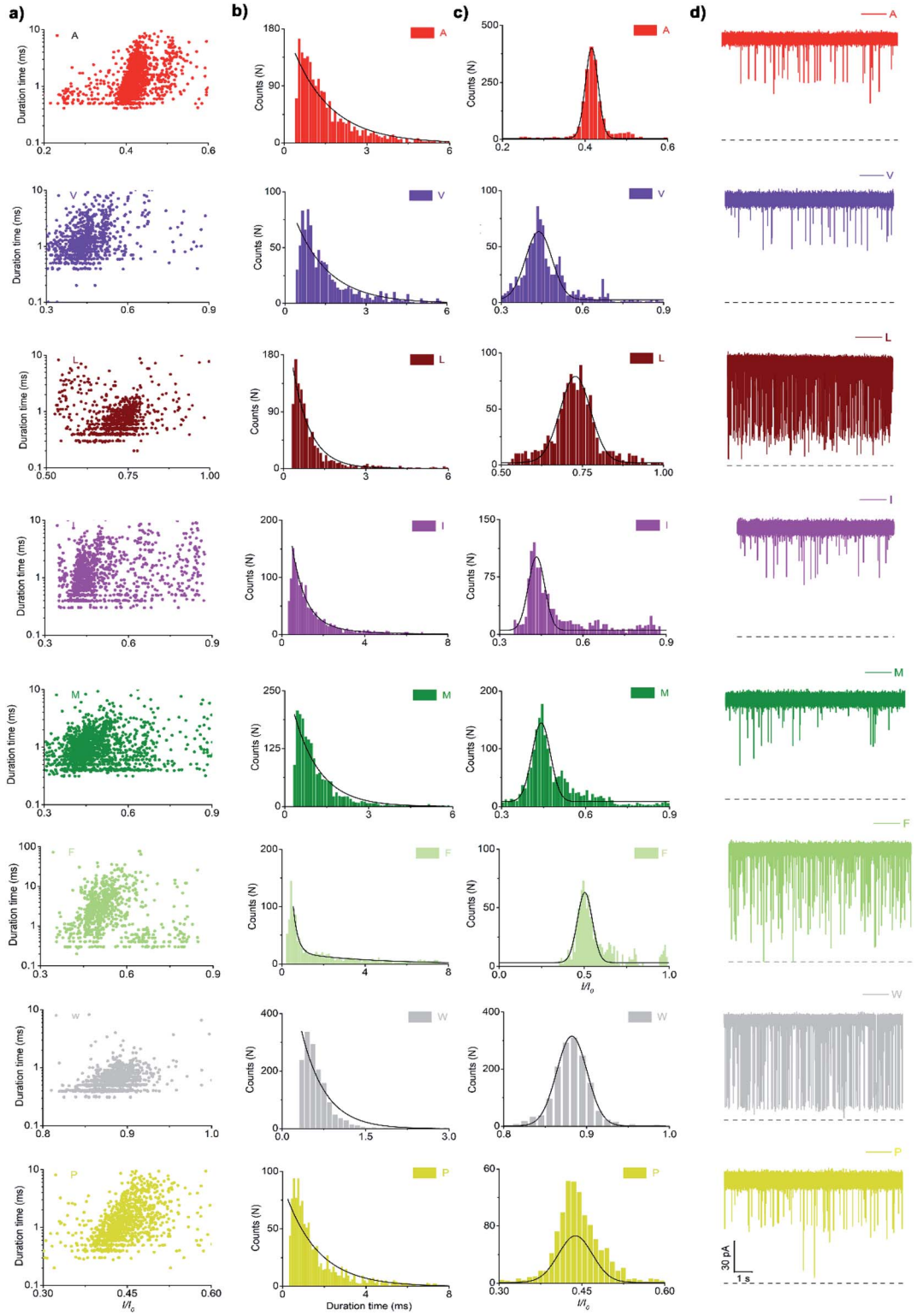

Fig. 2 Scatter plot (a), histograms of duration time (b), I/I_0 (c), and raw data (d) of the bipolar peptide probe containing nonpolar amino acids such as alanine (A), valine (V), leucine (L), isoleucine (I), proline (P), tryptophan (W), methionine (M), and phenylalanine (F) ($n = 1090$ (D_4AR_5), $n = 986$ (D_4VR_5), $n = 1107$ (D_4LR_5), $n = 1223$ (D_4IR_5), $n = 1381$ (D_4MR_5), $n = 1082$ (D_4FR_5), $n = 1214$ (D_4WR_5), $n = 1214$ (D_4PR_5) = 1215). The scatter plot of events shows current blockage I/I_0 *versus* duration time. The blockage amplitudes were fitted by Gaussian distribution, and the histograms of duration times were fitted by the exponential function.

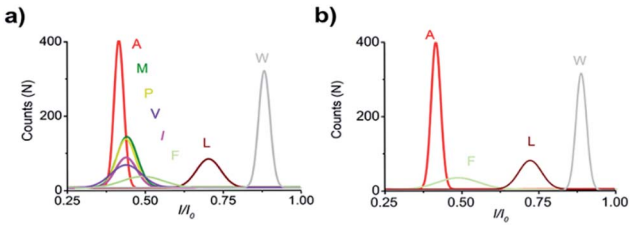

Fig. 3 Superimposed I/I_0 histograms of A, V, L, I, P, W, M, and F (a). I/I_0 histograms of A, F, L, and W (b). For each histogram, at least 1000 events were analysed, and the same applies to the figures below.

For the peptide probe D_6XR_5 (named X^-), the experimental process was the same as the procedure mentioned above, except that a constant voltage of +70 mV was applied to the *cis* compartment.

Results and discussion

Feasibility of the electrical recognition of proteinogenic amino acids using the aerolysin nanopore

For electrical recognition of the 20 proteinogenic amino acids using an aerolysin nanopore, bipolar peptide probes were

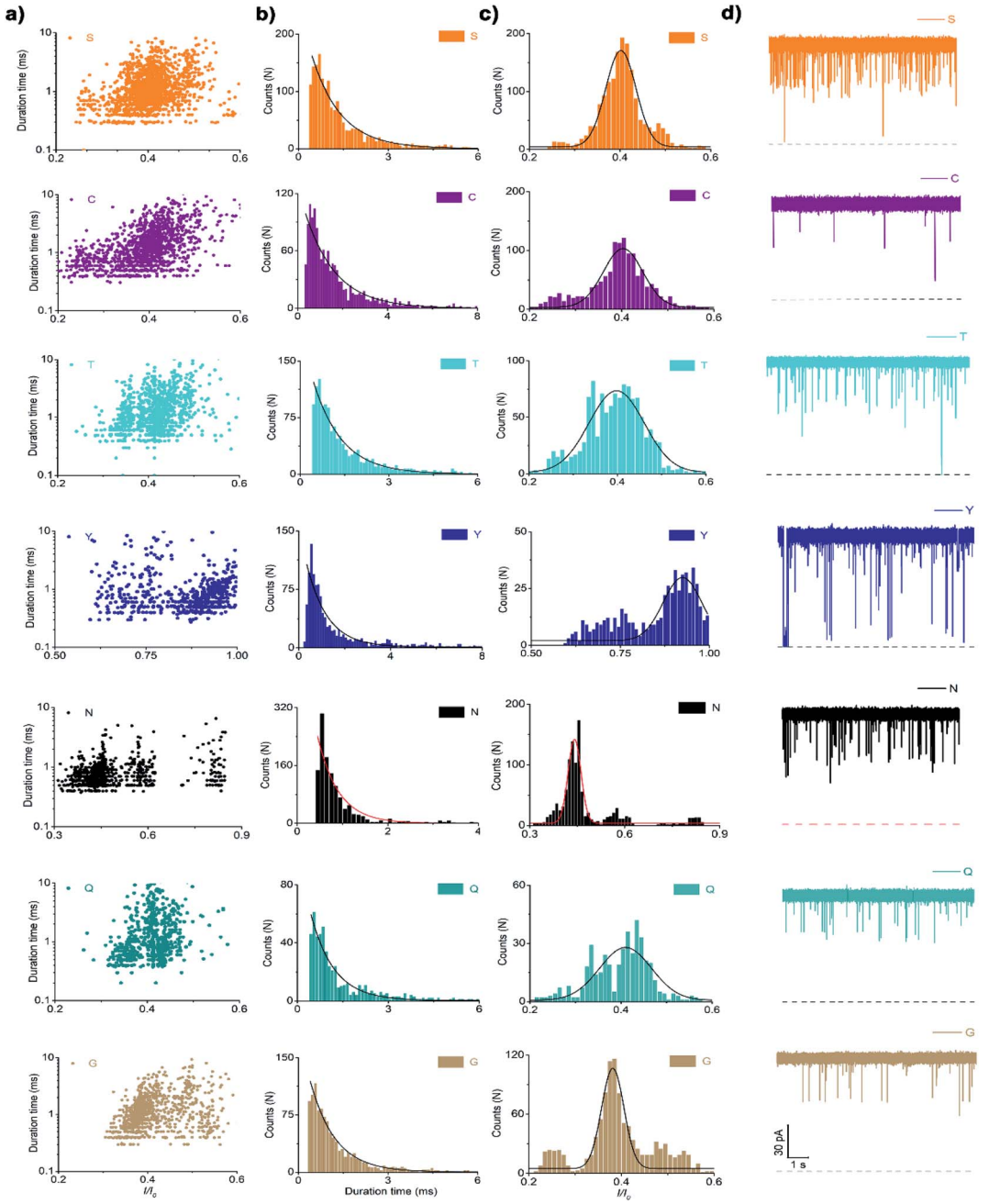

Fig. 4 Scatter plot (a), histograms of duration time (b), I/I_0 (c), and raw data (d) of the bipolar peptide probe containing polar uncharged amino acids such as glycine (G), serine (S), glutamine (Q), threonine (T), cysteine (C), asparagine (N), and tyrosine (Y) ($n = 1820$ (D_4SR_5), $n = 1412$ (D_4CR_5), $n = 1180$ (D_4TR_5), $n = 1077$ (D_4YR_5), $n = 1095$ (D_4NR_5), $n = 1068$ (D_4GR_5), $n = 1068$ (D_4QR_5)).

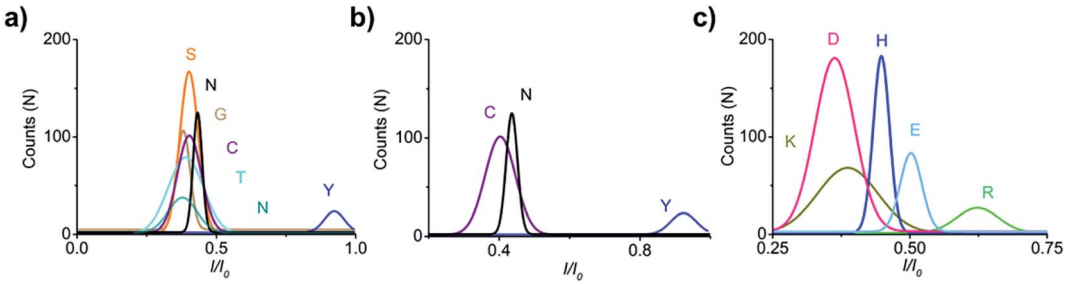

Fig. 5 Superimposed I/I_0 histograms of G, S, Q, T, C, N, and Y (a). I/I_0 histograms of C, N, and Y (b). Superimposed I/I_0 histograms of K, H, R, D, and E (c).

synthesised by linking D residues to the N-terminal and R residues to the C-terminal of individual amino acids (Fig. 1a).[38,39] An external positive voltage (70 mV) was applied to the *trans* side of the lipid bilayer(Fig. 1b). When the peptide passed through the aerolysin nanopore, transient blockade of the ionic current was observed (Fig. 1c). Each characteristic current blockade corresponded to the process of an individual peptide through the nanopore, and each peptide was recognized based on the blockage current and duration time. The feasibility of the assay was first tested by three groups of peptide probes (D_4XR_5, D_6XR_8, and D_8XR_{10}) to distinguish alanine (A), cysteine (C), and serine (S). In the case of D_4XR_5, all three peptides (D_4AR_5, abbreviated as A, D_4CR_5, abbreviated as C, D_4SR_5, abbreviated as S) produced several short single-level current signals (Fig. S1†). I_0 is defined as the open pore current for current amplitude analysis and I is defined as the blockage current when the analyte remained within the pore. Gaussian fitting (Fig. S1a†) revealed that A had the highest I/I_0 value.[40,41] The current signals produced by S were characterised by small spikes, whereas peptide C showed a jagged pattern (Fig. S1b†). In contrast, in the case of probe D_6XR_8 and D_8XR_{10}, there was no significant difference among the three peptides in any group (D_6XR_8: A6, C6, and S6; D_8XR_{10}: A8, C8, and S8) in terms of blocking degree, duration time, or signal shape (Fig. S1b†). Thus, the best identification was achieved with the bipolar probe D_4XR_5.

With the initial success, we set out to fully evaluate the potential of this strategy for the identification of all proteinogenic amino acids. Twenty D_4XR_5 peptides were divided into three groups according to the polarity of the side chain of amino acid X, namely, non-polar amino acid group, polar neutral amino acid group, and polar charged amino acid group. The group of non-polar amino acids comprised alanine (A), valine (V), leucine (L), isoleucine (I), proline (P), tryptophan (W), methionine (M), and phenylalanine (F). All these peptides produced current blocks when they passed through the aerolysin pore (Fig. 2d). Using statistical analysis, the distribution of blocking current was fitted to Gaussian functions and the duration time of the peptides was fitted by exponential distributions based on the first passage process[42,43] (Fig. 2a–c and 3a). Among those, the I/I_0 histograms of A, L, W, and F were located at 0.42 ± 0.0145, 0.70 ± 0.0140, 0.88 ± 0.0129, and 0.50 ± 0.0121, respectively, exhibiting four well-separated peaks (Fig. 3b). The current blockades and duration of the peptides containing V, I, P, and M were too close to be easily distinguished, most likely due to their similarities in spatial structures, volumes, or molecular weights.

In the case of the polar uncharged amino acid group, glycine (G), serine (S), glutamine (Q), threonine (T), cysteine (C), asparagine (N), and tyrosine (Y) were analysed under the same conditions as that of non-polar amino acids (Fig. 4 and 5a). Among those, the peptides containing C, N, and Y produced blockade populations distinct from one another (Fig. 5b), with the I/I_0 value of 0.39 ± 0.015, 0.44 ± 0.012, and 0.93 ± 0.048, respectively. The current amplitude and duration time distribution of G, S, Q, and T were too similar to be differentiated.

In the same way, the polar charged amino acid group contains three amino acids with positive charges, lysine (K), histidine (H), and R, and two amino acids with negative charges, D and glutamic acid (E). D_4XR_5 probes bearing them were identified *via* the nanopore assay (Fig. 6 and 5). Peptides H, R, and E could be well distinguished based on the degree of blocking, and the fitted values located in 0.45 ± 0.015 (H), 0.72 ± 0.012 (R), and 0.52 ± 0.011 (E), respectively (Fig. 5c). While the I/I_0 of D and K were too similar to be differentiated, their current blockades were clearly distinguished from those of H, R and E. Overall, with the help of a bipolar peptide probe, it was feasible to recognise proteinogenic amino acids using an aerolysin nanopore electrically. Bipolar probes containing A, F, L, W, C, N, Y, H, E, and R could be identified using I/I_0 and duration time, whereas the remaining 10 proteinogenic amino acids cannot be recognized.

In previous studies, the tug-of-war between positive and negative forces acting on the two oppositely charged tails of the dipolar peptide contributed to stretching the peptide and to increase the dwell time.[33–35] Consistent with what was observed for α-hemolysin pores in these reports, the dwell time of the dipolar peptides bearing H or W increases when the applied voltage increases from +50 to +80 mV (Fig. S2†).

Distinction of 9 of the 20 proteinogenic amino acids with the bipolar probe D_4XR_5

When grouped by the polarity of the side chain of X, a few amino acids could not be distinguished by the nanopore. We further aimed to examine if amino acids could be identified when not grouped (Fig. S3†). As shown in Fig. 8, I/I_0 histograms

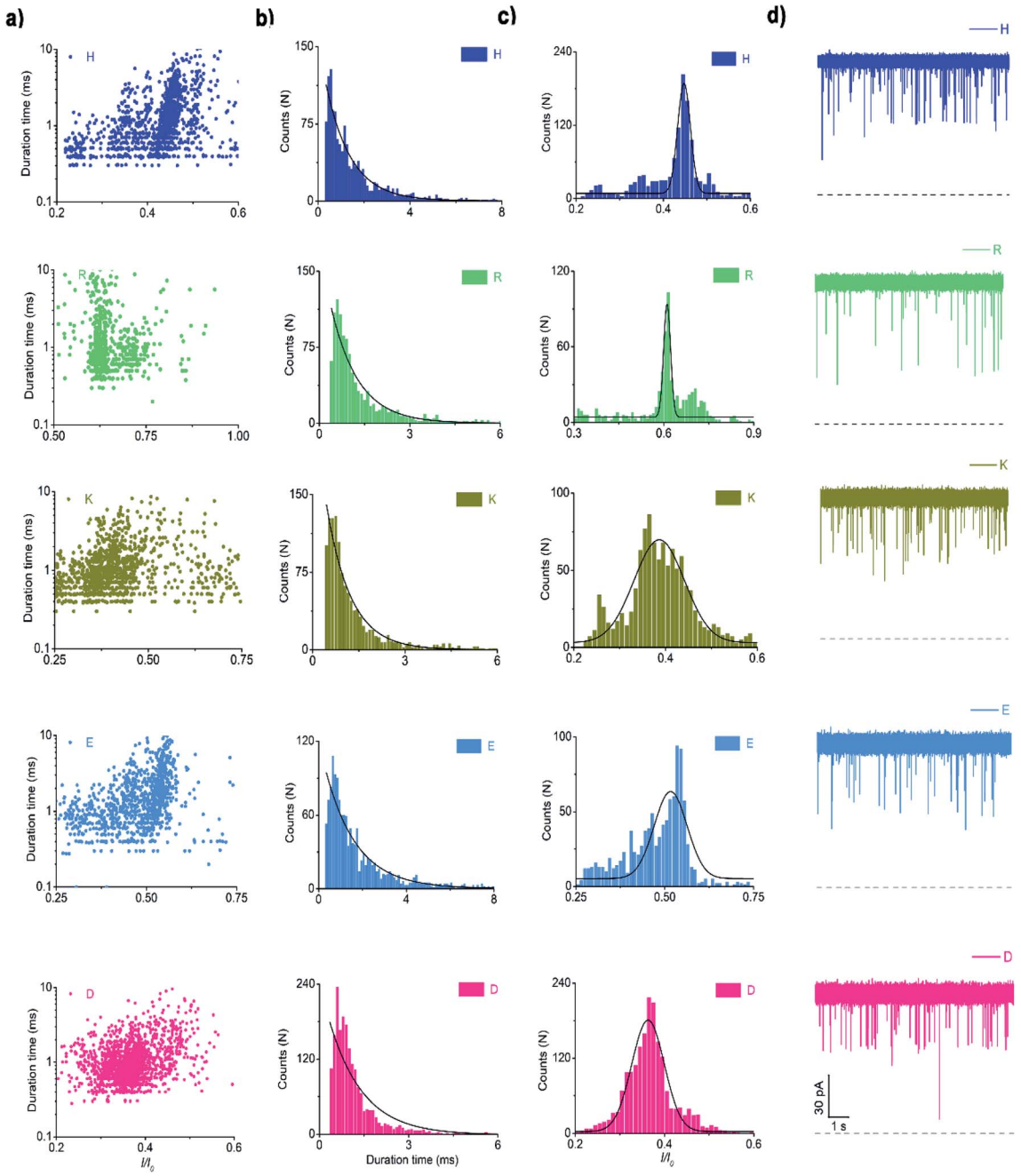

Fig. 6 Scatter plot (a), histograms of duration time (b), I/I_0 (c), and raw data (d) of the bipolar peptide probe bearing polar charged amino acids such as lysine (K), histidine (H), arginine (R), aspartic (D), and glutamic acids (E) ($n = 1420$ (D_4HR_5), $n = 1229$ (D_4KR_5), $n = 1090$ (D_4RR_5), $n = 1265$ (D_4ER_5), $n = 1529$ (D_4DR_5)).

of peptides D, M, E, R, L, W, and Y exhibited well-separated peaks (Fig. 7a). The duration times of the remaining 13 peptides were combined for exponential fitting, and N and A were distinguished (Fig. 7b). It is noteworthy that W and Y showed large I/I_0 (0.88 ± 0.0129 and 0.93 ± 0.0480), which may be attributed to the large side chain of an indole group or a phenol group.

To probe the mechanism underlying the blockade current, we plotted the relationship of the current amplitude against the volume of amino acids (Fig. 7c). Overall, the blocking current was found to increase as the volume of amino acid increased, which is largely consistent with the findings of H. Ouldali's study used a short polycationic carrier to identify amino acids.[30] However, there were notable exceptions in this study, such as A, D, T, Q, and K (Fig. S4†). We speculated that this may be related to the structures of the probes. We used the bipolar probe (D_4XR_5) with the target amino acid in the middle of the polypeptide chain, while H. Ouldali's group used the unipolar probe (XR_7) with the target amino acid at the N-terminal. Current blockades are likely to be affected by the position of the target

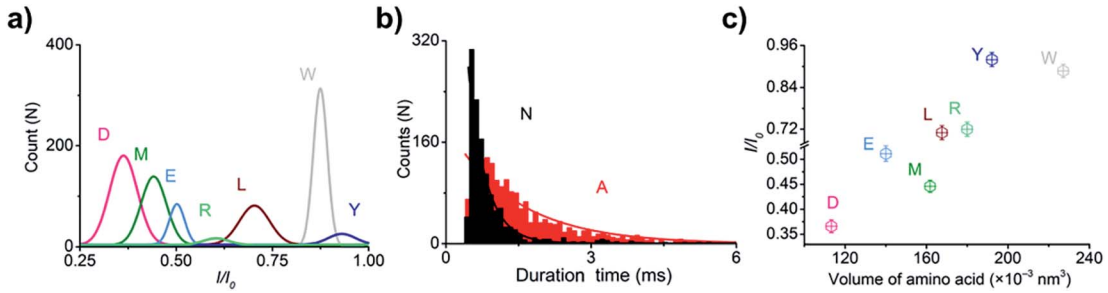

Fig. 7 Identification of proteinogenic amino acids *via* an aerolysin nanopore with the bipolar peptide probe D_4XR_5. (a) Identification of D, M, E, R, L, W, and Y based on the I/I_0 values. (b) Comparison of the duration times of A and N at +70 mV. (c) Relationship of current amplitude against volume of the seven amino acids.

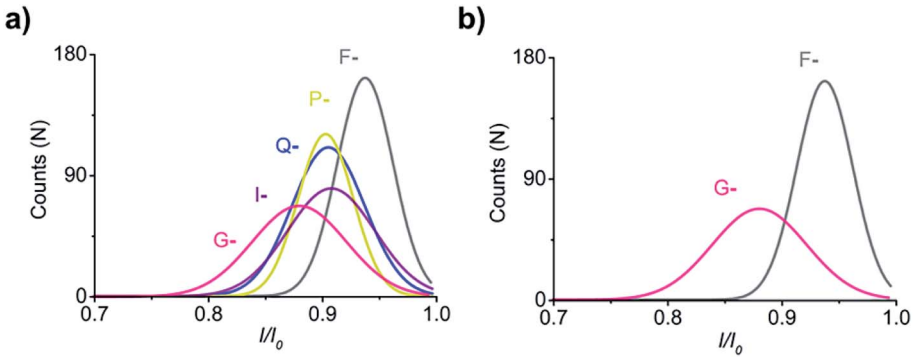

Fig. 8 Identification of the randomly selected five amino acids (I, F, G, P, and Q) using the negatively charged bipolar peptide probe D_6XR_5. (a) Histograms of I/I_0 values of I-, F-, G-, P-, and Q-. (b) Histograms of I/I_0 values of F-, and G-.

amino acid in the peptide and the probe sequence. The current amplitude (I/I_0) in our assay ranged from 0.35 to 0.93, whereas theirs lay within the range of 0.32–0.4. The variation range of I/I_0 in this study is much larger than theirs. On the other hand, in addition to the volume, the structure, charge properties of the side chain, and molecular masses of target amino acid also greatly influence the current signal. Different side chains will cause different non-covalent interactions between amino acids and nanopores, including electrostatic interactions, π-effect, and hydrophobic interactions. Previous reports of Long's group have also indicated that the steric hindrance effect is not a dominant factor for amino acid discrimination, in which the smaller cysteine produced the evident current signatures, while the larger asparagine and glutamine induced fast and undistinguishable current variations.[31]

Distinction of I, F, G, P, and Q employing the negatively charged probe D_6XR_5

To improve the ability of our strategy to recognise the remaining 11 amino acids, I, F, G, P, and Q were randomly selected as identification objects. The charge of peptides was reversed by adding two aspartic acid residues to the N-terminus of D_4XR_5, and the obtained probe D_6XR_5 (X-) was employed to distinguish the five amino acids. The negatively charged peptide was added to the *cis* side of the aerolysin chamber, and a positive voltage (70 mV) was applied to drive it into the aerolysin nanopore. In this case, the I/I_0 histograms of F- and G-exhibited well-separated populations (Fig. 8). Notably, compared with that of the positively charged peptides (D_4XR_5), the blocking degree of the negatively charged peptides (D_6XR_5) significantly increased (from 0.35–0.55 to 0.61–0.95). This result shows that changing the charge of the bipolar peptide probe can improve the ability of the aerolysin nanopore to distinguish amino acids, which may be attributed to the anionic selectivity of the aerolysin nanopore.[44,45] Previous studies have demonstrated that there are two positively charged amino acids located at the entrance of the pore and the bottom of the lumen in wild-type aerolysin.[46] This would produce strong electrostatic interactions between the peptide probe and the inner wall of the nanopore, significantly affecting the translocation of negatively charged peptides through the nanopore. As a result, the blocking degrees of negatively charged bipolar peptide probes are greatly increased, thus improving the ability of the aerolysin nanopore to distinguish different amino acids.

Conclusions

In the present work, we proposed a bipolar peptide probe to enable electrical recognition of proteinogenic amino acids using an aerolysin nanopore. The bipolar peptide probe was formed by linking aspartic acid residues to the N-terminal and arginine residues to the C-terminal of individual amino acids.

The advantage of this structure is that it contains amino acids with opposite charges, which is intended to improve the interaction between the probe and the inner wall of the nanopore, thus enhancing the ability to recognise amino acids. Among the 20 amino acids, our strategy permitted the reliable identification of 9 amino acids, based on distinct current blockades and duration times. In the case of the positively charged peptide probe D_4XR_5, amino acids D, M, E, R, L, W, and Y were effectively identified by current blockages, and N and A could be distinguished by duration times. Furthermore, the ability to distinguish peptides can be improved by employing the negatively charged probe D_6XR_5 (X-), as proved by the identification of G, and F. It is speculated that this is due to the strong electrostatic interactions caused by the positively charged residues at the entrances and inside the lumen during the translocation of the aerolysin nanopore. In our future study, we will include all types of peptides with a negatively charged probe. Recently, Long *et al.* pioneered in designing a series of mutant aerolysin that modulates charge distribution *via* site-directed mutagenesis.[32] Inspired by this, we could design a specific biological nanosensor with a high resolution to identify amino acids in the future. We anticipate that the development of mutant aerolysin, combined with the bipolar peptide probe, would facilitate the application of aerolysin nanopores in the identification of proteinogenic amino acids.

Author contributions

D. X. conceived the work. Y. G., M. C., and Q. Z. performed the experiments. D. X., Y. G., M. C., and Q. Z. analysed the data. D. X., Y. G. and Y. W. wrote the manuscript. All authors discussed the results and commented on the manuscript.

Conflicts of interest

There are no conflicts to declare.

Acknowledgements

This research was supported by the National Natural Science Foundation of China (21874062, 22076073), Collaborative Innovation Center in Universities of Shandong Province (Linyi University), the Natural Science Foundation of Shandong Province (ZR2017ZC0226), Key Research and Development Program of Linyi City (2021030), and the Open Project Foundation of Shandong (Linyi) Institute of Modern Agriculture, Zhejiang University (No. ZDNY-2021-FWLY02012).

Notes and references

1 L. Liu and H. C. Wu, *Angew. Chem., Int. Ed. Engl.*, 2016, **55**, 15216–15222.
2 D. Xi, J. Shang, E. Fan, J. You, S. Zhang and H. Wang, *Anal. Chem.*, 2016, **88**, 10540–10546.
3 B. Wei, N. Liu, J. Zhang, X. Ou, R. Duan, Z. Yang, X. Lou and F. Xia, *Anal. Chem.*, 2015, **87**, 2058–2062.
4 D. Xi, Z. Li, L. Liu, S. Ai and S. Zhang, *Anal. Chem.*, 2018, **90**, 1029–1034.
5 M. Cui, Y. Ge, X. Zhuge, X. Zhou, D. Xi and S. Zhang, *Chin. J. Chem.*, 2021, **39**, 2035–2043.
6 D. Branton, D. W. Deamer, A. Marziali, H. Bayley, S. A. Benner, T. Butler, M. Di Ventra, S. Garaj, A. Hibbs, X. Huang, S. B. Jovanovich, P. S. Krstic, S. Lindsay, X. S. Ling, C. H. Mastrangelo, A. Meller, J. S. Oliver, Y. V. Pershin, J. M. Ramsey, R. Riehn, G. V. Soni, V. Tabard-Cossa, M. Wanunu, M. Wiggin and J. A. Schloss, *Nat. Biotechnol.*, 2008, **26**, 1146–1153.
7 A. Meller and D. Branton, *Electrophoresis*, 2002, **23**, 2583–2591.
8 I. M. Derrington, T. Z. Butler, M. D. Collins, E. Manrao, M. Pavlenok, M. Niederweis and J. H. Gundlach, *Proc. Natl. Acad. Sci. U. S. A.*, 2010, **107**, 16060–16065.
9 E. Kennedy, Z. Dong, C. Tennant and G. Timp, *Nat. Nanotechnol.*, 2016, **11**, 968–976.
10 Q. Liu, Y. Wang, Y. Liu, H. Wang, W. Li, P. Tang, T. Weng, S. Zhou, L. Liang, J. Yuan, D. Wang and L. Wang, *Nanoscale*, 2020, **12**, 19711–19718.
11 G. M. Roozbahani, X. Chen, Y. Zhang, L. Wang and X. J. S. M. Guan, *Small Methods*, 2020, **4**, 2000266.
12 W. L. Hsu and H. Daiguji, *Anal. Chem.*, 2016, **88**, 9251–9258.
13 L. Mereuta, M. Roy, A. Asandei, J. K. Lee, Y. Park, I. Andricioaei and T. Luchian, *Sci. Rep.*, 2014, **4**, 3885.
14 H. Wang, W. Huang, Y. Wang, W. Li, Q. Liu, B. Yin, L. Liang, D. Wang, X. Guan and L. Wang, *ACS Sens.*, 2021, **6**, 3781–3788.
15 M. Li, W. Li, Y. Xiao, Q. Liu, L. Liang, D. Wang, W. Huang and L. Wang, *Biosens. Bioelectron.*, 2021, **194**, 113602.
16 H. Chae, D. K. Kwak, M. K. Lee, S. W. Chi and K. B. Kim, *Nanoscale*, 2018, **10**, 18423.
17 W. Qiu and E. Skafidas, *ACS Appl. Mater. Interfaces*, 2014, **6**, 16777–16781.
18 D. Rodriguez-Larrea and H. Bayley, *Nat. Nanotechnol.*, 2013, **8**, 288–295.
19 B. Cressiot, A. Oukhaled, L. Bacri and J. Pelta, *Bionanoscience*, 2014, **4**, 111–118.
20 G. Oukhaled, J. Mathe, A. L. Biance, L. Bacri, J. M. Betton, D. Lairez, J. Pelta and L. Auvray, *Phys. Rev. Lett.*, 2007, **98**, 158101.
21 E. L. Bonome, F. Cecconi and M. Chinappi, *Nanoscale*, 2019, **11**, 9920–9930.
22 W. Si and A. Aksimentiev, *ACS Nano*, 2017, **11**, 7091–7100.
23 H. Y. Wang, Y. L. Ying, Y. Li, H. B. Kraatz and Y. T. Long, *Anal. Chem.*, 2011, **83**, 1746–1752.
24 Y. X. Hu, Y. L. Ying, Z. Gu, C. Cao, B. Y. Yan, H. F. Wang and Y. T. Long, *Chem. Commun.*, 2016, **52**, 5542–5545.
25 A. B. Farimani, M. Heiranian and N. R. Aluru, *npj 2D Mater. Appl.*, 2018, **2**, 1–9.
26 G. Di Muccio, A. E. Rossini, D. Di Marino, G. Zollo and M. Chinappi, *Sci. Rep.*, 2019, **9**, 6440.
27 G. Zollo and A. E. Rossini, *Nanoscale Adv.*, 2019, **1**, 3547–3554.
28 Z. Chen, Z. Wang, Y. Xu, X. Zhang, B. Tian and J. Bai, *Chem. Sci.*, 2021, **12**, 15750–15756.

29 F. Piguet, H. Ouldali, M. Pastoriza-Gallego, P. Manivet, J. Pelta and A. Oukhaled, *Nat. Commun.*, 2018, **9**, 966.
30 H. Ouldali, K. Sarthak, T. Ensslen, F. Piguet, P. Manivet, J. Pelta, J. C. Behrends, A. Aksimentiev and A. Oukhaled, *Nat. Biotechnol.*, 2020, **38**, 176–181.
31 B. Yuan, S. Li, Y. L. Ying and Y. T. Long, *Analyst*, 2020, **145**, 1179–1183.
32 S. Li, X. Y. Wu, M. Y. Li, S. C. Liu, Y. L. Ying and Y. T. J. S. M. Long, *Small Methods*, 2020, **4**, 2000014.
33 A. Asandei, M. Chinappi, J. K. Lee, C. Ho Seo, L. Mereuta, Y. Park and T. Luchian, *Sci. Rep.*, 2015, **5**, 10419.
34 A. Asandei, M. Chinappi, H. K. Kang, C. H. Seo, L. Mereuta, Y. Park and T. Luchian, *ACS Appl. Mater. Interfaces*, 2015, **7**, 16706–16714.
35 M. Chinappi, T. Luchian and F. Cecconi, *Phys. Rev. E: Stat., Nonlinear, Soft Matter Phys.*, 2015, **92**, 032714.
36 Z. Gu, Y. L. Ying, C. Cao, P. He and Y. T. Long, *Anal. Chem.*, 2015, **87**, 907–913.
37 N. Zhang, Y.-X. Hu, Z. Gu, Y.-L. Ying, P.-G. He and Y.-T. Long, *Chin. Sci. Bull.*, 2014, **59**, 4942–4945.
38 A. Asandei, A. E. Rossini, M. Chinappi, Y. Park and T. Luchian, *Langmuir*, 2017, **33**, 14451–14459.
39 A. Asandei, G. Di Muccio, I. Schiopu, L. Mereuta, I. S. Dragomir, M. Chinappi and T. J. S. M. Luchian, *Small Methods*, 2020, **4**, 1900595.
40 W. Li, Y. Wang, Y. Xiao, M. Li, Q. Liu, L. Liang, W. Xie, D. Wang, X. Guan and L. Wang, *ACS Appl. Mater. Interfaces*, 2022, **14**, 32948–32959.
41 Y. Xiao, J. Ren, Y. Wang, X. Chen, S. Zhou, M. Li, F. Gao, L. Liang, D. Wang, G. Ren and L. Wang, *Biosens. Bioelectron.*, 2022, **212**, 114415.
42 J. Li and D. S. Talaga, *J. Phys.: Condens. Matter*, 2010, **22**, 454129.
43 S. Redner, *A Guide to First-Passage Processes*, Cambridge University Press, 2001, vol. 8, p. 252.
44 S. Li, C. Cao, J. Yang and Y. T. Long, *ChemElectroChem*, 2019, **6**, 126–129.
45 F. Hu, B. Angelov, S. Li, N. Li, X. Lin and A. Zou, *Chembiochem*, 2020, **21**, 2467–2473.
46 C. Cao, Y. L. Ying, Z. L. Hu, D. F. Liao, H. Tian and Y. T. Long, *Nat. Nanotechnol.*, 2016, **11**, 713–718.